Journal of Environmental Management 375 (2025) 124396

Contents lists available at ScienceDirect

Journal of Environmental Management

journal homepage: www.elsevier.com/locate/jenvman

Research article

Vacuum ultraviolet radiation from gaseous plasma for destruction of water contaminants

Mark Zver [a,b], Rok Zaplotnik [a], Miran Mozetič [a], Alenka Vesel [a], Arijana Filipić [c], David Dobnik [c], Belisa Alcantara Marinho [d], Gregor Primc [a,*]

[a] Department of Surface Engineering, Jozef Stefan Institute, Jamova Cesta 39, 1000, Ljubljana, Slovenia
[b] Jožef Stefan Post Graduate School, Jamova Cesta 39, 1000, Ljubljana, Slovenia
[c] Department of Biotechnology and Systems Biology, National Institute of Biology, Večna Pot 111, 1000, Ljubljana, Slovenia
[d] Department for Nanostructured Materials, Jožef Stefan Institute, Jamova 39, 1000, Ljubljana, Slovenia

ARTICLE INFO

Keywords:
Water treatment
Viruses
Antibiotics
Dyes
Bacteria
Low-pressure plasma V-UV irradiation
OH● radicals

ABSTRACT

Innovative technological solutions are needed for water decontamination to combat the diverse pollutants present in water systems, as no single optimal decontamination technique is appropriate for all circumstances. Vacuum-ultraviolet (V-UV) radiation is a source of energetic photons that break molecular bonds, producing a plethora of chemically reactive agents, most notably OH● radicals, which can cause the degradation of harmful pollutants. Low-pressure gaseous plasma is a good source of V-UV radiation; however, its application to liquid water poses challenges. We constructed an inductively coupled radiofrequency plasma to produce high-intensity V-UV radiation, which was applied to contaminated water via a V-UV-transparent window. Plasma was sustained in hydrogen, as it produces the highest V-UV intensity among all gases at selected discharge parameters. Bacteriophage MS2 was used as an indicator of microbial decontamination efficiency. Reactive oxygen and nitrogen species were measured at various treatment setups to quantify their effect on MS2 inactivation and elucidate the primary inactivation factors. At optimal conditions, the concentration of active virus dropped by 9 $\log_{10}$ PFU/mL in 60 s. The optimal experimental setup was then used to treat bacteria *E. coli*, *S. aureus*, antibiotic tetracycline, and synthetic dye methylene blue as representatives of other types of pollutants, all of which were effectively removed/degraded within 10 min of treatment. A comparison of energy efficiency (EEO) to other disinfection setups was made for bacteriophage inactivation. With a low EEO value, we showcase the potential of this technique for further work in this field.

1. Introduction

Plasma is referred to as the fourth state of matter and is generated when sufficient energy is applied to a gas, causing ionisation of gas molecules, producing a highly reactive mixture of ions, electrons, radicals, atoms, and photons. Artificially generated gaseous plasma discharges are widely used in commercial applications such as semiconductor manufacturing (Kanarik, 2020), photovoltaics (Schlemm et al., 2005), surface treatment for adhesion improvement (Förster, 2022), thin layer deposition (Gosar et al., 2020), cutting or welding (Venkatramani, 2002), and much more. The high versatility of plasma treatment techniques stems from the various discharge setups (plasma jet, arc discharge, dielectric barrier discharge) and operating parameters (pressure, working gas, input power, frequency), which can produce a variety of reactive particles for useful applications. In the case of radiofrequency (RF) plasma discharges, oscillation of free electrons is caused by the applied RF field, resulting in ionisation of atoms and subsequent gas breakdown or plasma discharge (Chabert et al., 2021). RF discharges can be capacitively or inductively coupled. The latter discharge generally displays significantly higher electron densities and is used in plasma propulsions, plasma lighting, or as a source of negative ions beams (Chabert et al., 2021). Inductively coupled plasmas are also characteristically able to transit between E-mode or H-mode, each with its unique plasma properties and discharge parameters. When plasma is sustained with a lower power input, the E-mode prevails, where the induced electric field is negligible compared to the voltage drop between the coil and the chamber wall (in our case, glass tube). In this case, plasma is characterised by low electron density, relatively high electron

* Corresponding author.
E-mail address: gregor.primc@ijs.si (G. Primc).

https://doi.org/10.1016/j.jenvman.2025.124396
Received 26 October 2024; Received in revised form 20 January 2025; Accepted 29 January 2025
Available online 4 February 2025

temperature, and weak light emission. When more power is absorbed, the plasma shifts into an inductive coupling regime, termed H-mode. The transition can be observed visually, as the H-mode discharge is significantly more luminous and has approximately two orders of magnitude higher electron density (Zaplotnik et al., 2011). To generate the highest possible amount of V-UV radiation for the purpose of water disinfection, the latter mode would be preferred, but one should also consider the required energy input as it relates to the operating costs of such treatments.

V-UV photons, with wavelengths between 100 and 200 nm, possess sufficient energy to break molecular bonds, which can be utilised for improving wettability (Vesel et al., 2023), sterilisation (D. Wang et al., 2010), gas and water treatment (M. C. Gonzalez and Braun, 1995; Ochiai et al., 2013). In water treatment applications, V-UV can directly interact and disrupt organic molecules, or it can act indirectly by generating $OH^{\bullet}$ (Eqs. (1) and (2)), which disrupt organic molecules via hydrogen abstraction, electrophilic addition, or electron transfer reactions (Eqs. (3)–(5)) (M. G. Gonzalez et al., 2004; Legrini et al., 1993). Water treatment processes utilising $OH^{\bullet}$ for pollutant degradation are called advanced oxidation processes (AOP).

$$H_2O + h\nu(\langle 190nm) \rightarrow H^{\cdot} + HO^{\cdot} \quad (1)$$

$$H_2O + h\nu \rightarrow H^{+} + e^{-} + HO^{\cdot} \quad (2)$$

$$HO^{\cdot} + RH \rightarrow R^{\cdot} + H_2O \quad (3)$$

$$HO^{\cdot} + PhX \rightarrow HOPhX^{\cdot} \quad (4)$$

$$HO^{\cdot} + RX \rightarrow RX^{\cdot +} + HO^{-} \quad (5)$$

In Equations (3)–(5), R and RX represent an organic substrate, $R^{\bullet}$ and $RX^{\bullet}$ an organic radical, while PhX and $HOPhX^{\bullet}$ present the nucleophile and the product of electrophilic addition, respectively. The amount and intensity of V-UV photons generated by a plasma discharge are dependent on many factors, such as working gas, operating pressures, input power etc. (Zaplotnik et al., 2011). V-UV radiation being efficiently absorbed by almost all material, including oxygen molecules in the air, means that specific setups using vacuum systems must be utilised to allow them to interact with the treated substance (D. Wang et al., 2010).

In the water purification application of V-UV radiation had been previously used for the degradation of pollutants such as natural organic matter (Buchanan et al., 2004), chemicals (W. Han et al., 2004; Imoberdorf and Mohseni, 2011; Krakkó et al., 2021, 2022; Ochiai et al., 2013), bacteria (Krakkó et al., 2021; Liu and Ogden, 2010; Ochiai et al., 2013), bacterial spores (Halfmann et al., 2007), and viruses (Moldgy et al., 2020; Ochiai et al., 2013). However, all authors used V-UV sources different from hydrogen plasma, such as medium-pressure mercury lamps, LED lights, or excimer lamps, with rather narrow waveband emissions, which can only interact with certain molecules. Some authors reported synergistic effects between different light sources (Matafonova and Batoev, 2022; Ramsay et al., 2000). Therefore, it would be reasonable to assume that a V-UV source emitting a richer radiation spectrum could more efficiently degrade a greater variety of contaminants from water.

In this article, we present a unique experimental setup with a radiofrequency inductively coupled plasma reactor (ICP), which can produce rather intense V-UV radiation in a range of wavelengths between about 150 and 200 nm (photon energy 6–8 eV) and applied it to liquid samples. We quantified the concentration of $OH^{\bullet}$ in polluted water and evaluated their contribution towards MS2 bacteriophage (MS2) inactivation by systematically excluding competing biocidal agents. The characterization of treatment was finalized by performing an energy efficiency comparison with similar methods.

Expanding further from bacteriophage treatment, Gram-negative bacteria *E. coli*, antibiotic tetracycline, and a massively produced synthetic dye methylene blue were also treated with the system. These were selected as model representatives of waterborne bacterial disease outbreaks (M. N. V. Prasad and Grobelak, 2020), accumulating pharmaceutical contamination (Amangelsin et al., 2023), and harmful industrial runoff (Oladoye et al., 2022), respectively. By their rapid inactivation/degradation, we showcase the ability to treat different types of pollutants and provide a proof-of-concept to utilize such devices in practical applications.

2. Materials and methods

2.1. Inductively coupled low-pressure RF plasma system and sample treatment chamber

The plasma device used in this study is an inductively coupled plasma (ICP) system (Fig. 1) powered by an RF generator Cesar 1320

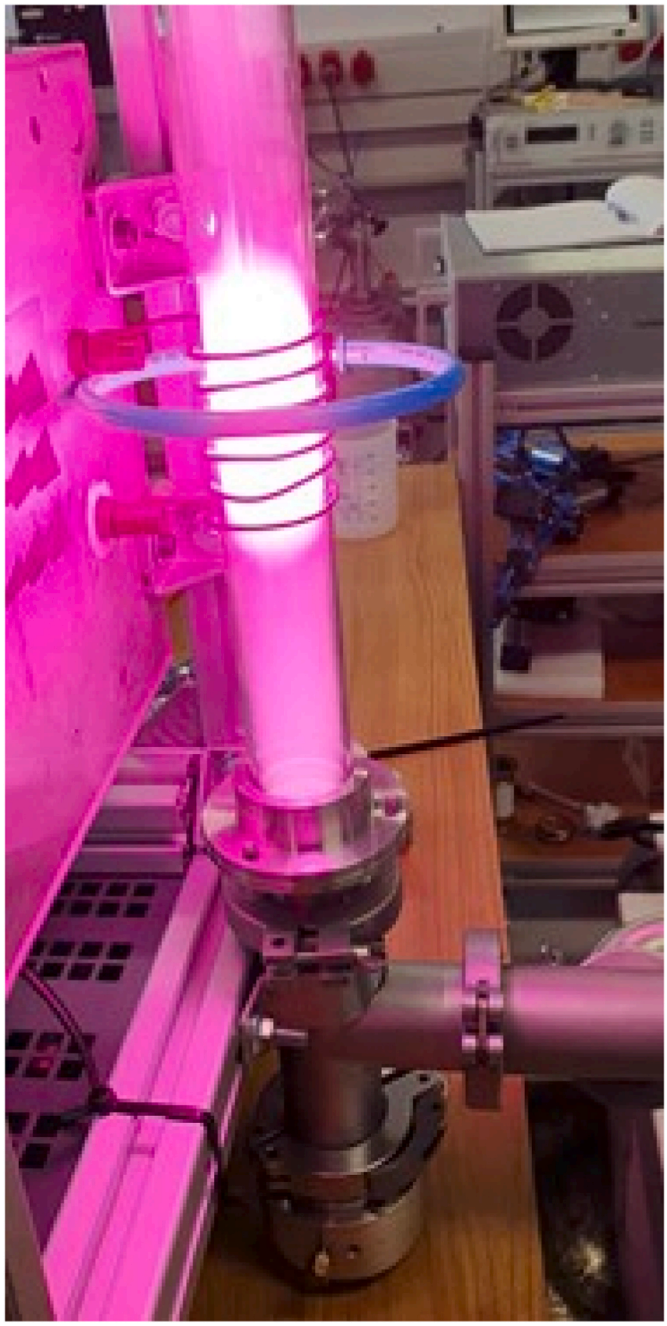

Fig. 1. A photograph of the plasma system with plasma in the H-mode.

(Advanced Energy, USA), connected to a copper coil positioned around the centre of the discharge chamber. The input voltage and current waveforms were sine waves with a frequency of 13.56 MHz. For the parameters most frequently used in this research 50 W and 390 W of real power, the RMS voltages were 900 V_{RMS} and 1010 V_{RMS}, respectively. The discharge chamber consists of a borosilicate glass tube with a length and diameter of 30 and 4 cm, respectively. The tube was evacuated to a base pressure of 1 Pa with a two-stage rotary vane pump Trivac D40B (Leybold, Germany). Pressure was measured with a capacitive absolute pressure transducer Baratron 722A (MKS Instruments, USA), and the H_2 gas was leaked into the tube via mass flow controller Aera MFC FC-7700 (Advanced Energy, USA) (Fig. 2). Here, it should be stressed that the plasma generated in this system was used only as a source of radiation, especially V-UV radiation, and was not in contact with the polluted water. To apply V-UV radiation to liquid samples in atmospheric conditions, a special chamber was constructed, as describer previously (Zver et al., 2025). Briefly, an aluminium chamber with a radiation-facing MgF_2 window, which is transparent to wavelengths down to about 110 nm, was utilised to contain a hermetically sealed glass petri dish, which contained the liquid sample at atmospheric pressure. The chamber also allows for the exchange of atmospheric gases via the two valves positioned on either side of the chamber and the use of an optional, non-hermetic radiation barrier. The barrier is used to obscure the treated sample from direct V-UV radiation. The radiation can produce reactive gaseous species above the barrier (headspace), which can subsequently diffuse to the liquid surface by passing through the gaps between the barrier and the sample chamber. Nitrogen does not absorb V-UV radiation down to around 110 nm (Tigrine et al., 2016), while oxygen present in the air does so efficiently (Watanabe et al., 1953), producing ozone in the process, which could aid in the disinfection process, while also enabling easier operation of the system from a practical application viewpoint. When required, the gas inside the chamber was exchanged with N_2 by fitting a tube on the side valve and allowing the desired gases to flow through the chamber for 30 s, after which the valves were closed on both sides, and the tube was subsequently removed. The chamber containing the prepared sample was then attached to the bottom of the ICP plasma system, and the treatment would proceed for up to 10 min. In some cases, the glass petri dish was non-hermetically covered with a radiation barrier (black-painted aluminium sheet), preventing direct V-UV interaction with the liquid sample, while still allowing the reactive species to reach the liquid sample surface. In other cases, 200 mM of D-mannitol was added to act as a scavenger for $OH^{\bullet}$, excluding them from interacting with contaminants. The distance between the MgF_2 window and the liquid surface was always 3 cm.

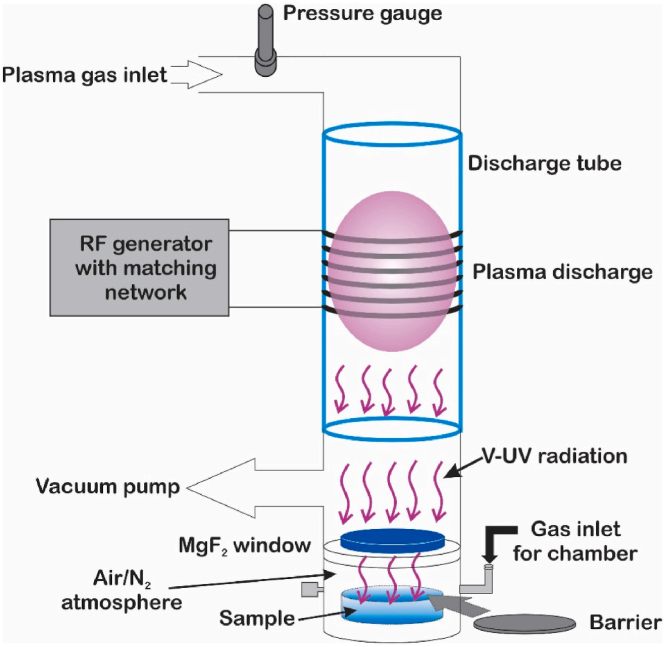

Fig. 2. Schematic presentation of the plasma treatment of samples.

2.2. V-UV spectrometry

Emission radiated from ICP plasma was measured with VS7550 V-UV to NIR Mini-Spectrograph (Resonance Ltd., Canada). The device has a UHV MgF_2 window and a laminar flow purge system, through which a steady flow of N_2 gas was established to prevent radiation absorption by the ambient atmosphere. The spectrometer has a Czerny-Turner configuration, where slit size, input aperture (F#), order sorting filters, grating angle, and dark exposures can be controlled with VS7550 Spectrometer software. It allows light intensity measurements ranging from 104 to 1000 nm. In all measurements presented in this work, a 100 μm slit, a 1200 L/mm grating, F8.4 aperture, a −4° grating angle, and 6−500 ms integration time were used. The distance between the plasma-generation area and the V-UV spectrometer was always 30 cm. Based on the spectroscopic measurements of V-UV radiation (Fig. 4), the optimal V-UV radiation was emitted in ICP plasma with H_2 gas at approximately 20 Pa either in E-mode or H-mode, at a real power input of 50 W or 390 W, respectively.

2.3. Virus inactivation experiments and spot-titre plaque assay

For treating viruses in solution, 2 mL of Milli-Q (MQ) water with bacteriophage MS2 was placed in the glass petri dish (water layer thickness of 1.1 mm) inside the chamber with the initial concentration of 9 $\log_{10}$ PFU/mL and sealed with the MgF_2 window cover. The contribution to virus inactivation from V-UV radiation, ozone, and $OH^{\bullet}$ in solution were systematically excluded by using a non-hermetic radiation barrier, nitrogen atmosphere, and adding 200 mM of D-mannitol to the solution, respectively. The treatment conditions were as follows: plasma in either E-mode (50 W) or H-mode (390 W), plasma in H-mode + radiation barrier (B), and plasma in H-mode + 200 mM mannitol (M).

For MS2 quantification, a modified version of the double-layer agar (DAL) method, previously described by Beck et al. (N. K. Beck et al., 2009), was used. All growth media referred to in this method consist of Trypticase Soy Broth (BD BBL™) medium, supplemented with 1.93 g/L $MgCl_2 \times 6H_2O$ (Sigma-Aldrich, USA) and 100 mg/L ampicillin sodium salt (Gibco™, USA), with varying concentrations (%) of bacteriological agar (Biolife, Agar Bios Special LL, USA). An amount of 100 μL of overnight *E. coli* CB390 culture, grown in a liquid medium, was inoculated into 5 mL of dissolved agar (0.7 %) medium, which was then mixed and poured over solid medium (1.5 %) plates. After 15 min, 10-μL droplets of virus sample dilutions were spotted on the plates (at least 4 per sample) that were placed lid-up in an incubator overnight at 37 °C. The number of plaques was counted the following day, and the number of infectious viruses was quantified by considering the sample dilutions using the following equations:

$$Virus\ concentration : log\left(\bar{x} \times 10^{d \times log\ 4}\right) \quad (6)$$

$$Log\ stdev : \sqrt{\frac{1}{n} \times \sum (logx_i - log\bar{x})^2} \quad (7)$$

where $\bar{x}$ denotes the average of counted plaques, d the dilution step, n the number of measurements, and *log4* represents the 4x dilution factor used for the experiment. All treatments were performed in triplicates. The control samples underwent the same procedure without the ignition of plasma.

2.4. Plasma-activated water MS2 disinfection

To evaluate the contribution of long-lived reactive species (H_2O_2, O_3, NO_2^-) to MS2 inactivation, an experiment was conducted by using plasma-activated (treated) water (PAW). PAW was prepared in the same manner as for the virus-inactivation experiments explained previously, without adding MS2 into the water. The water samples were all treated for the maximum duration of 10 min, after which 1 mL of the treated PAW was placed into a 1.5 mL tube, and MS2 bacteriophage was added to it at the initial concentration of 9 $\log_{10}$ PFU/mL. After a 10-min incubation period, a dilution series was made, and the samples were spotted on agar plates, which was the same as described above. A one-way ANOVA analysis with a confidence interval of 0.05 was performed to reveal statistically different treatment outcomes. The liquids were treated with V-UV radiation in either nitrogen or air atmosphere inside the sample chamber. The treatment conditions were as follows: plasma in either E-mode (50 W) or H-mode (390 W), plasma in H-mode + radiation barrier (B), and plasma in H-mode + 200 mM mannitol (M). The quantity of long-lived reactive species (H_2O_2, O_3) was measured with a commercial water quality testing device, Palintest Photometer 7500BT (Palintest, UK), using the appropriate testing reagents. The temperature and pH of the liquid remained consistent throughout the treatment procedure (25 °C, pH = 7), as measured by Palintest Multi-parameter pocket sensor (Palintest, UK).

2.5. OH• radical quantification

A terephthalic acid (TA) assay was used to determine the amount of $OH^\bullet$ in water solution. TA reacts with $OH^\bullet$ in solution, producing 2-hydroxyterephthalic acid (HTA), which emits a fluorescent signal at 425 nm when excited with monochromatic laser radiation at 318 nm. A 5 mM solution of TA (Sigma-Aldrich, USA) was prepared by preheating MQ water to 80 °C and using 1 M NaOH to adjust the pH to 11 before adding TA during mixing. Additionally, to study the degradation profile of generated HTA, a 0.5 mM (100 mg/L) solution of HTA (Merck KGaA, Germany) was prepared by dilution with sterilised MQ water, and treating 2 mL samples, quantifying remaining HTA as described above. A glass petri dish containing 2-mL samples was placed inside the sample treatment chamber for treatments with V-UV radiation from plasma. A radiation barrier, N_2 gas, or mannitol was inserted when required and irradiated with plasma as described above for the indicated amount of time. After treatment, a 200 μL sample was transferred to a 96-well plate (Brand, pureGrade™ S, Germany), and fluorescence measurements were performed with a spectrometer Infinite 200 Pro (Tecan, Switzerland) at 75 gain. During the treatment of the TA solution, the HTA is formed, but at the same time it is also degraded. Therefore, in order to determine the actual production rate of the HTA and, consequently, of the $OH^\bullet$, a deconvolution had to be made between the measured HTA and HTA degradation curve (Zver et al., 2025). To do so, only HTA was treated to determine the degradation curve. The deconvoluted curve was then convoluted back with a constant, i.e., without a degradation. Because not every $OH^\bullet$ is used to form one HTA, the production rate of HTA is the lower value of the $OH^\bullet$ production rate.

2.6. Energy efficiency calculations

Besides disinfection effectiveness and consumer and environmental safety, a water treatment technique must also be cost-effective for implementation in practice (Bolton et al., 2001). Based on its working principle, plasma-generated V-UV irradiation is classified as an advanced oxidation process (AOP), relying on *in situ* generation of reactive oxygen and nitrogen species (RONS) to achieve disinfection of polluted water. Since electric energy represents the majority of operating costs for most AOPs, a standard approach to estimate the price-performance of AOPs is to calculate the energy efficiency per order (EEO, Equation (8)), defined as the energy, expressed in kWh, required to reduce the concentration of a contaminant by one order of magnitude (1 $\log_{10}$) in a unit of volume (1 m^3).

$$EEO\left(\frac{\text{kWh}}{\text{m}^3\cdot\text{order}}\right)=\frac{\textit{Power input}\ (\text{kW})\times\textit{Treatment time}\ (\text{h})}{\textit{Volume}\ (\text{m}^3)\times 1\ \textit{log}_{10}} \quad (8)$$

2.7. Pollutant degradation experiments

To evaluate the performance of the system towards other types of pollutants, the optimal treatment parameters, namely H-mode hydrogen plasma with air as the atmosphere in the sample chamber, were used to treat Gram-negative (G^-) *Escherichia coli* (EC, NCTC 12923, bioMérieux S.A., France) and Gram-positive (G^+) *Staphylococcus aureus* (SA, NCTC 10788, bioMérieux S.A., France) bacteria, as well as the antibiotic tetracycline (TETR, Sigma-Aldrich, 98.0–102.0% HPLC, USA) and an organic dye methylene blue (MB, Thermo Fisher Scientific, USA), for up to 10 min.

E. coli and *S. aureus* cultures were inoculated into liquid TSB medium and incubated in a shaker (200 rpm, 37 °C, 24h). The bacteria were harvested by three progressions of centrifugation (5 min, 5000 rpm) and washing with MQ water before being serially diluted, spread onto TSB plates, and incubated at 37 °C overnight. The following day, the bacteria were counted to prepare a sample solution of ~8 $\log_{10}$ bacteria for experiments with plasma-emitted V-UV radiation. The same counting method was utilised to quantify bacterial survival by plating 100 μL of sample dilutions on TSB agar plates, incubating them overnight at 37 °C, and subsequently enumerating the colonies.

For TETR degradation experiments, a 10 mg/L solution was prepared by dissolving TETR powder in MQ water. The solution was stirred overnight by a magnetic stirrer. As described above, 2-mL samples were placed in the glass petri dish and treated with plasma, followed by adding 100 μL of methanol to prevent further reactions. The samples were analysed by Liquid Chromatography (LC) using a Waters Acquity UPLC I-Class Plus System equipped with a photodiode array detector (PDA) at 25 °C. The reverse-phase column used was a Waters Acquity UPLC® BEH C18 (1.7 μm) 2.1 × 150 mm column. The equipment was operated in continuous mode using as mobile phase 70% of water/methanol/0.1 M oxalic acid with ratios of 80:10:10 (v/v) and 30% acetonitrile. The flow rate was 0.3 mL/min. Samples of 10 μL were injected and the retention time was 1.5 min. The limits of quantification and detection were 0.034 and 0.010 mg/L of TETR, respectively, at 357 nm.

MB was dissolved in MQ water at a concentration of 100 mg/L, treated with plasma as described above, and the degradation was measured by absorbance reduction at 664 nm.

For all pollutant treatments, 2-mL samples were placed in the glass petri dish and treated with plasma as described above. All experiments were conducted in triplicates for the indicated amount of time, and the average concentration and standard deviation were calculated.

3. Results and discussion

3.1. V-UV intensity

In our previous work, we confirmed that H_2 gas emits the most intense V-UV radiation (Zver et al., 2025). A typical spectrum of ICP hydrogen plasma used in this study is presented in Fig. 3. Intense radiation can be seen in wavelengths below 300 nm. The continuum above 190 nm arises from continuum a−b molecular transitions. However, the most intense radiation is due to the Lyman (B−X) and Werner (C−X) molecular band transitions. In order to compare radiation intensity at different discharge parameters, we integrated emitted light intensity in the V-UV region (from 100 to 200 nm).

Since plasma gas pressure and input power are the primary factors affecting plasma discharge characteristics, we modulated these two parameters to obtain the optimal conditions for highly intense V-UV

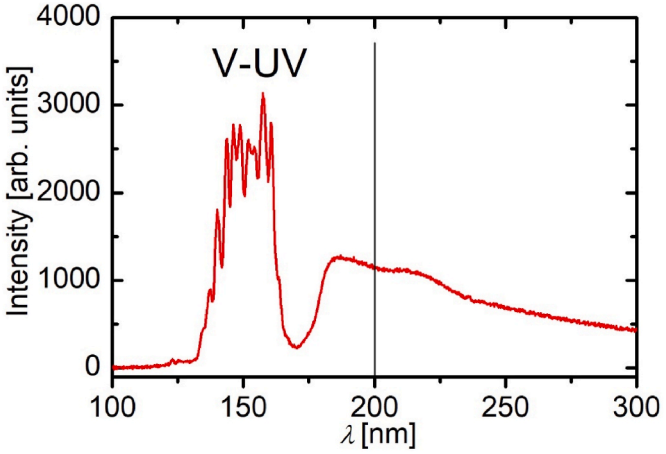

Fig. 3. A typical spectrum of ICP hydrogen plasma.

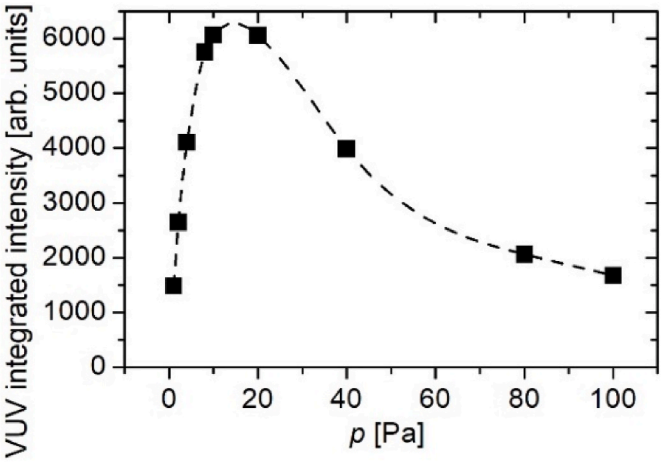

Fig. 4. Pressure-dependent V-UV intensity of H_2 plasma at 50 W real power.

radiation. At least 50 W was required to obtain a stable E-mode plasma, which we used as our starting point. We then incrementally increased the H_2 gas flow (pressure) and kept the pumping speed constant to identify the maximum V-UV intensity. As can be seen in Fig. 4, the maximum V-UV radiation from plasma generated at the absorbed real power of 50 W in an ICP plasma system was achieved at pressures around 20 Pa, which is explained by two contradictory effects. At low pressures, the electron density increases with increasing pressure because of the reduced loss of the charged particles at walls due to the increasing collision frequency and, thus, decreasing diffusion. The increasing electron density causes more excitations and, thus, more intensive radiation. At elevated pressure, on the other hand, the electron temperature starts decreasing with increasing pressure because of numerous collisions; hence, the lower electron temperature causes inefficient ionisation and excitation of radiative states. There are optimal conditions in between, evidently at the pressure of 20 Pa when using our experimental setup. When additional power is supplied to the system, the radiation increases with increasing power, and eventually, plasma discharge transforms from E-mode (predominant capacitive coupling) to H-mode (predominant inductive coupling), which characteristically produces more intense radiation. This can be seen in Fig. 5, where integrated V-UV radiation intensity is displayed versus the real RF power. Here, 'real RF power' denotes reflected power subtracted from forwarded power, where both values are measured by the RF generator.

For further treatments and experiments, 20 Pa and 50 W and 390 W of real RF power for E- and H-mode were used, because these were the

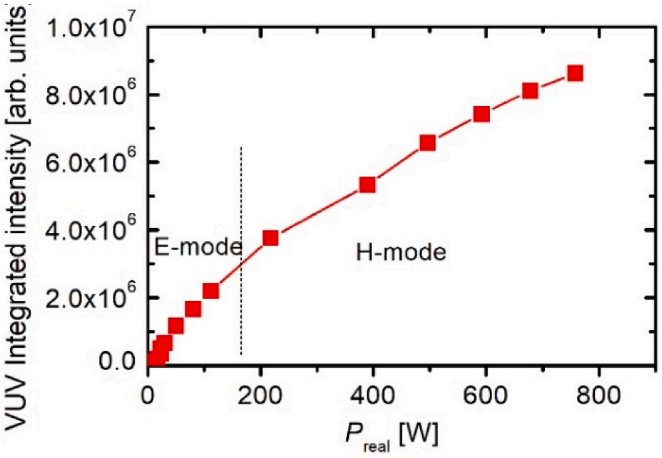

Fig. 5. Integrated V-UV radiation intensity of 20 Pa H_2 plasma versus the real power.

lowest powers where each mode was stable.

3.2. Virus inactivation

A comparison between E- and H-mode hydrogen plasma was performed to establish the power-dependent virus inactivation efficiency. These were performed with either air or N_2 inside the sample chamber to elucidate the contribution of direct V-UV water treatment (N_2 atmosphere) while excluding the contribution of any reactive oxygen species (air atmosphere) generated in the headspace of the sample treatment chamber.

As can be seen in Fig. 6, the presence of oxygen inside the sample chamber (because nitrogen was replaced with air) improves the overall bacteriophage inactivation efficiency when illuminated with V-UV radiation arising from hydrogen plasma in both E- and H-modes. Interestingly, hydrogen plasma in the E-mode with air atmosphere (black circles in Fig. 6) in the sample treatment chamber achieved total inactivation slightly faster than hydrogen plasma sustained in the H-mode in the nitrogen atmosphere (red squares in Fig. 6).

The MS2 inactivation shown in Fig. 6 could be explained by different efficiencies in $OH^{\bullet}$ production in water when using nitrogen or air atmospheres in the sample treatment chamber. The contribution of various reactants was evaluated by systematically excluding the main inactivation agents, which are V-UV radiation, reactive oxygen species,

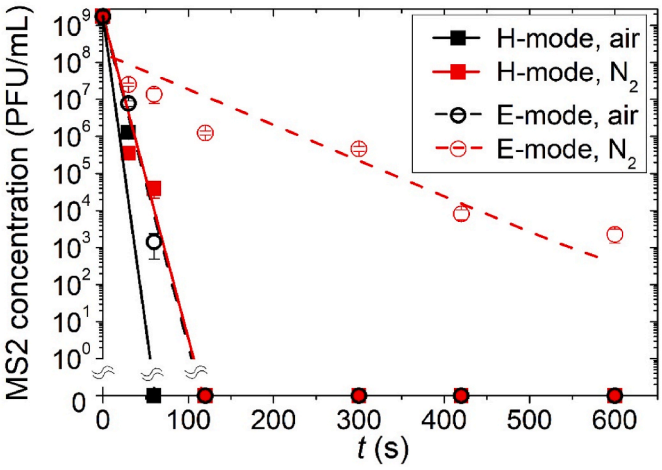

Fig. 6. MS2 bacteriophage inactivation by hydrogen ICP plasma ignited in H-mode (squares) and E-mode (circles) in either air (black colour) or nitrogen (red colour) atmosphere.

and $OH^{\bullet}$, by utilising a non-hermetic radiation barrier, nitrogen atmosphere, and a mannitol solution, respectively. When air is exchanged for nitrogen (Fig. 7) in the sample chamber, there is a clear drop in inactivation efficiency, confirming the role of reactive oxygen species in virus inactivation. The virus inactivation was extremely slow or practically non-existent when a barrier was inserted into the nitrogen-containing chamber (Fig. 7 (a)). The radiation barrier was used to protect the water from direct V-UV radiation from plasma. The reactive species formed by plasma radiation in the sample's treatment chamber headspace were able to reach the liquid surface by passing through the sides of the barrier. Such an experiment removed the direct effect of V-UV plasma radiation on the water sample. When mannitol was added to the solution, the inactivation rate was reduced, but total inactivation was still achieved after 5 min of treatment, meaning that $OH^{\bullet}$ is not the only reactant responsible for virus inactivation.

However, treating the samples in an air atmosphere shows that other agents (not only $OH^{\bullet}$) are responsible for bacteriophage inactivation (Fig. 7 (b)). Most notable is the use of a V-UV barrier, where total inactivation was achieved after 7 min of treatment, even when the sample was completely obscured from the V-UV radiation. The addition of mannitol provided similar but slightly better results when compared to the nitrogen atmosphere in the sample's treatment chamber headspace. This indicates that when V-UV interacts with oxygen molecules in the sample's treatment chamber headspace, long-lasting reactive oxygen species are produced that can migrate to and react with the liquid, achieving virus inactivation without requiring direct irradiation of the polluted water with V-UV radiation. Therefore, oxygen inside the treatment chamber is beneficial to the overall plasma V-UV treatment performance.

3.3. PAW virus inactivation

Antimicrobial long-lived RONS, mainly H_2O_2 and O_3 (M. C. Gonzalez and Braun, 1995), are produced and dissolved in water during plasma V-UV irradiation. Their contribution to MS2 inactivation was evaluated by exposing MS2 bacteriophage to PAW. Both water treatment and virus exposure were set to 10 min. Additionally, the aforementioned RONS were measured using a photometric test.

For all the treatment conditions presented in Fig. 8, the measured NO_2 quantities were below the method's detection limit (>1.0 mg/L). For O_3 and H_2O_2 measurements, the only standouts were PAW treated in H-mode in an air atmosphere, which produced 1.6 ± 0.2 mg/L H_2O_2, and PAW treated in H-mode with the addition of mannitol (M) with 2.27 ± 0.7 mg/L O_3 detected. All other samples contained less than 0.3 mg/L for both disinfectants. Mannitol is a scavenger of $OH^{\bullet}$, which is involved in upstream and downstream reactions for generating RONS (Goldstein and Czapski, 1984). Thus, providing a scavenger that reacts with $OH^{\bullet}$ and reduces the pool of reactants, which is expected to achieve less virus inactivation. Moreover, excluding the $OH^{\bullet}$ from the reaction mixture significantly improved the production of O_3, indirectly aiding the inactivation efficiency.

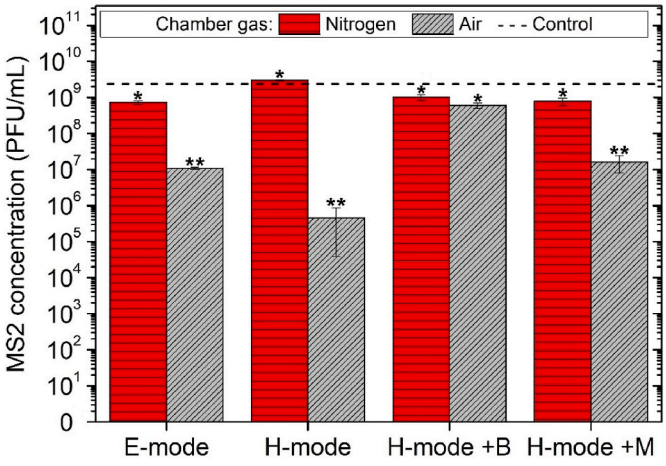

Fig. 8. MS2 bacteriophage exposed to plasma-activated water (produced by a 10-min plasma treatment) for 10 min; * and ** indicate statistically significant differences between treatments ($p < 0.05$).

Fig. 8 shows that only about 3 $\log_{10}$ inactivation was achieved by treating MS2-polluted water with PAW prepared in H-mode plasma with air in the sample's treatment chamber headspace. An expected decrease in viral inactivation was observed at lower powers used to sustain hydrogen plasma (E-mode). When nitrogen was present in the sample's treatment chamber headspace, fewer reactive oxygen species were produced and dissolved in PAW, resulting in no inactivation of MS2. Since $OH^{\bullet}$ reacts with and degrades long-lived H_2O_2 and O_3 (Legrini et al., 1993; Reisz et al., 2003), adding mannitol to the water sample may raise their concentration in PAW. On the other hand, when a plasma radiation barrier was implemented to prevent direct V-UV interaction with water, no significant virus inactivation was observed, even with the presence of air in the chamber. This indicates that V-UV radiation increases the production of long-lived RONS in the liquid and can be achieved by a complex system of intermediate reactions between short- and long-lived RONS, indirectly affecting the production and transport of the latter to the liquid phase, reviewed by several authors (Anderson et al., 2016; Hoigné and Bader, 1976; Jiang et al., 2014; Legrini et al., 1993; Zhou et al., 2020).

Z.-C. Yang et al., 2024 reported that an O_3 concentration of 4.8 mg/L was required to inactivate 4 $\log_{10}$ of MS2 in deionised water, while a H_2O_2 concentration of 850 mg/L was required for the same effect (Z.-C.

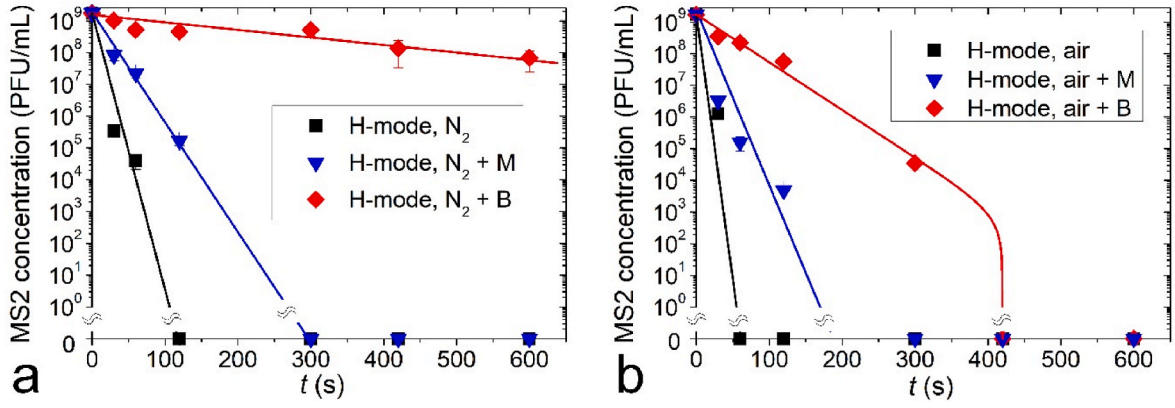

Fig. 7. MS2 bacteriophage inactivation in nitrogen (a) and air (b) atmosphere. B in the legend denotes that a radiation barrier was used, while M denotes that mannitol was used as an $OH^{\bullet}$ scavenger in the treated sample.

Yang et al., 2024). A concentration of 0.1 mg/L O_3 caused an MS2 reduction by 1 $\log_{10}$ in 3 min exposure time, and the inactivation did not seem to continue after that time (J. Fang et al., 2014). However, the inactivation was markedly improved by additional UV exposure, which was explained by the co-generation of $OH^{\bullet}$ from O_3 interaction with UV. Similarly, less than 1 $\log_{10}$ inactivation was observed when 5 mg/L H_2O_2 was used to treat MS2, while a combined UV/H_2O_2 process resulted in over 7 $\log_{10}$ inactivation, supposedly by the same effect (Sherchan et al., 2014). Due to a variety of factors affecting disinfection efficiency, it is difficult to compare results from different treatments directly; however, based on the published results, only the concentrations of O_3 for H-mode + mannitol (M) treatment are sufficient to explain the observed MS2 inactivation presented in Fig. 8. For clarity, a summary of key inactivation factors from various plasma treatments is presented in Fig. 9.

3.4. $OH^{\bullet}$ radical quantification

The results discussed above show that the major factor for virus inactivation in water treated by V-UV from hydrogen plasma are $OH^{\bullet}$ radicals. Therefore, we performed systematic measurements to quantify the concentration of $OH^{\bullet}$ in water samples by applying a TA assay. When $OH^{\bullet}$ is produced through a water homolysis reaction (Equation (1)) (M. G. Gonzalez et al., 2004), some react with TA to produce HTA, and the concentration of HTA can be measured with a spectrophotometer. However, HTA can also be degraded by the co-generated ozone when air is used in the sample's treatment chamber headspace (Zver et al., 2025), meaning that a degradation measurement is also needed to quantify generated HTA accurately. Fig. 10 shows the measured HTA signal when either TA or HTA solution was irradiated with V-UV from H_2 plasma, ignited at 50 W (E-mode) or 390 W (H-mode) at 20 Pa.

Again, the difference between E- and H-mode is immediately apparent since only the latter treatment caused total degradation of HTA within the designated treatment time. Knowing this, it is easier to interpret the curves of the TA irradiation experiments, which trend downwards after the initial upward progression. Using the results of our measurements (Fig. 10), one can estimate the $OH^{\bullet}$ production rate for each treatment condition. For that purpose, the formation and degradation curves presented in Fig. 10 were deconvoluted, and the deconvoluted signal was then convoluted back with a constant response, i.e., without degradation. In this way, only an HTA formation rate without any degradation is determined. Fig. 11 presents the HTA formation rate curves during irradiation with V-UV arising from hydrogen plasma sustained in E-mode and H-mode in either air or nitrogen in the sample's treatment chamber headspace. The results correlate perfectly with the results of MS2 inactivation presented in Fig. 6. The most significant $OH^{\bullet}$ production rate was when H-mode plasma was used as the V-UV source and air was in the sample's treatment chamber headspace, whereas the lowest production rate was when E-mode plasma was used, and the sample's treatment chamber headspace was filled with nitrogen.

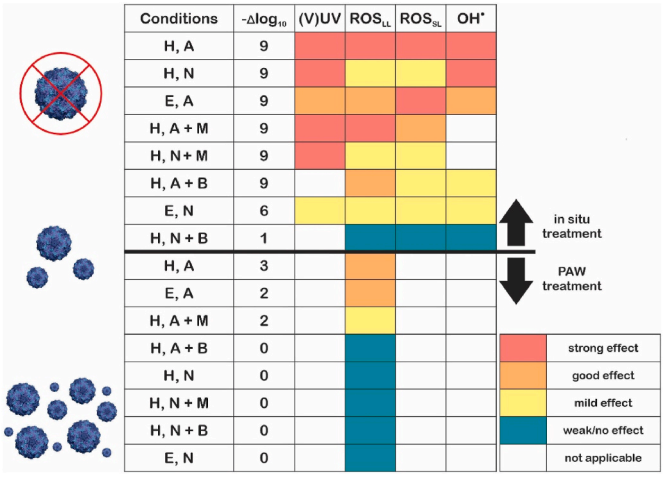

Fig. 9. Visual representation of major factors affecting MS2 inactivation with plasma treatment. (V)UV denotes V-UV and UV radiation, ROS_{LL} denotes long-lived ROS (O_3, H_2O_2); ROS_{SL} denotes short-lived ROS (O, $^1O_2$, O_2^-), excluding $OH^{\bullet}$; H denotes plasma in the H-mode; E denotes plasma in the E-mode; A denotes air used in the sample's treatment chamber headspace, while N denotes nitrogen; M denotes use of $OH^{\bullet}$ scavenger mannitol; B denotes the use of a non-hermetic radiation barrier; $-\Delta\log_{10}$ denotes a logarithmic change in virus infectivity.

Previous studies reported $OH^{\bullet}$ production rates in the ranges of 10^{-8}–10^{-10} M/s (Joshi et al., 1995; Kanazawa et al., 2011; Sahni and Locke, 2006), which is somewhat lower than production rates between 3.2 and 0.082 ± 0.04 × 10^{-6} M/s obtained from our setup. Here, we should stress again that the lines presented in Fig. 11 do not present the actual $OH^{\bullet}$ production rates but rather the HTA formation rates, which are related to $OH^{\bullet}$ production rate; therefore, they do not represent the total amount of $OH^{\bullet}$ produced. Nevertheless, the observed production rates still indicate a good performance of this setup regarding $OH^{\bullet}$ production.

3.5. Energy efficiency estimation

An extensive review comparing energy efficiency per order (EEO) estimations of different advanced oxidation processes was presented by Miklos et al. (2018), which led to categorisation into three groups based on median EEO values: <1 kWh/m^3, 1–100 kWh/m^3, and >100 kWh/m^3. The most energy-efficient system was ozonation with 0.15 kWh/m^3, followed by introducing UV treatment to the ozonation process at 0.2 kWh/m^3, while plasma processes fell into the second group with around 3.3 kWh/m^3 median EEO value. The decontamination efficiency was almost exclusively evaluating chemical contaminants, which behave differently from microbes. Nevertheless, it gives us something to compare the efficiency of our system. Here, it should be mentioned that some caveats are necessary to evaluate the applied V-UV radiation despite its sub-optimal application. Namely, even though the applied power of 50 W and 390 W were used to sustain the plasma in E- and H-mode, respectively, it must be stated that the radiation had dissipated in all directions (Fig. 1) of the discharge tube and only a small fraction of the plasma-emitted V-UV photons reached the sample. This fraction was calculated as a ratio between the solid angle of the plasma radiation impinging on the liquid in the sample chamber and the solid angle of the whole sphere. Approximately only 0.1 % of the plasma emitted V-UV light was actually used in these experiments, which was accounted for in the EEO calculation. Various plasma systems that used MS2 as a water decontamination target are also presented in Table 1, providing the most objective comparison between plasma discharges. The amount of V-UV light used for water treatment requires many optimisations, but the estimations in Table 1 indicate that the overall efficiency could be economical after optimisation of the treatment system. Furthermore, low-pressure plasmas can be sustained in large volumes at the specific power (power per unit volume of plasma) as low as about 1 W/liter (Gosar et al., 2020) so upscaling the experimental results reported in this scientific article looks feasible.

It can be seen that the best-performing methods (O_3, O_3/H_2O_2, UV lamps) also have applications in large water treatment setups. Relatively high EEO values are calculated for atmospheric-pressure plasma discharges, which is explained by a lower production of RONS, V-UV, and UV, as a large portion of energy is lost to heating the gas (Tendero et al., 2006). On the other hand, the low-pressure ICP system studied in this article achieves quite promising EEO values, with the E-mode discharge with an air atmosphere being the most energy-efficient technique among those probed in our experiments. The simultaneous application of powerful UV and V-UV radiation, along with a plethora of RONS generated due to the oxygen in the atmosphere, is sufficient for 9 $\log_{10}$

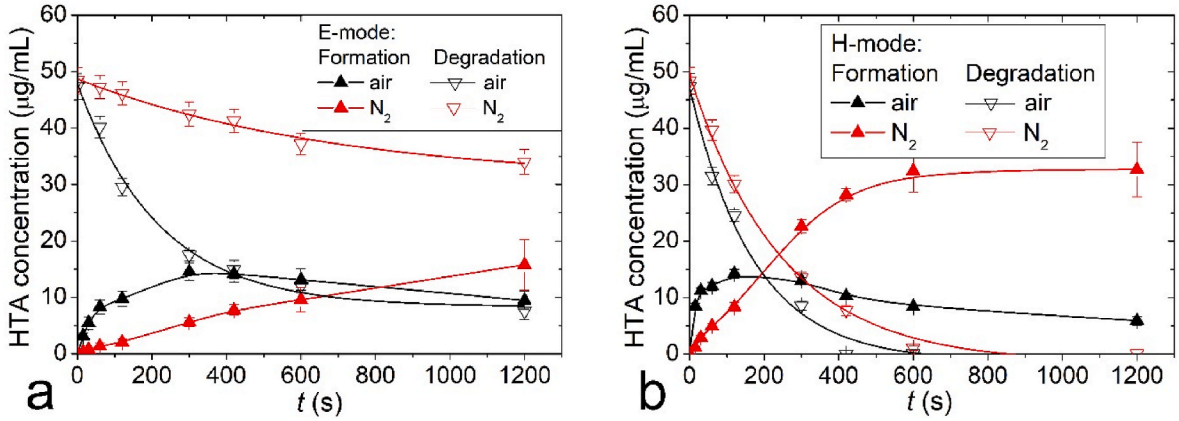

Fig. 10. HTA formation (upward triangles) and degradation (downward triangles) after plasma irradiation in E-mode (a) or H-mode (b) in either air (black line) or nitrogen (red line) atmosphere in the sample treatment chamber headspace.

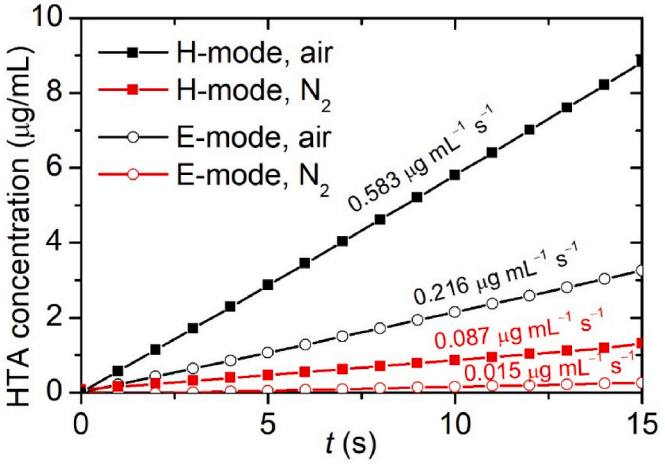

Fig. 11. HTA formation during E-mode and H-mode plasma irradiation treated in either air or nitrogen atmosphere.

Table 1
Energy efficiency per order for MS2 inactivation in water. Ozonation and O_3/H_2O_2 added for 'best-in-class' comparison.

System	EEO (kWh/m^3/order)	Reference
Ozonation	0.15	Miklos et al. (2018)
O_3/H_2O_2	0.2	Miklos et al. (2018)
Plasma jet	1166.67	(Y. Wu et al., 2015)
Streamer corona discharge	311.11	Lee et al. (2011)
Dielectric barrier discharge	5.21	Guo et al. (2018)
UV-C LED 260/280 nm	2.022	(S. E. Beck et al., 2017)
Low-pressure UV lamp	0.028	(S. E. Beck et al., 2017)
Medium-pressure UV lamp	0.06	(S. E. Beck et al., 2017)
KrCl excimer lamp 222 nm	0.05	Hull and Linden (2018)
ICP plasma, E-mode, N_2	0.66	This work
ICP plasma, E-mode, air	0.07	This work
ICP plasma, H-mode, N_2	0.57	This work
ICP plasma, H-mode, air	0.30	This work

inactivation of MS2 within a minute of treatment time, requiring nearly eight times less energy input than the treatment with plasma in the H-mode. Again, it needs to be stated that the values calculated in this article only represent the 0.1 % of energy applied to the sample itself, and many optimisations of the technology still need to be done.

3.6. General aspects of pollutant degradation using V-UV radiation from hydrogen plasma

In the preceding sections, we proved the degradation efficiency of viruses when using V-UV radiation from hydrogen plasma and explained the mechanisms involved. The method, however, is applicable for destroying many other organic pollutants in water since the $OH^{\bullet}$ readily interact with any organic matter, causing the formation of radicals (Equation (3)) and irreversible oxidation by forming organic radicals (Equation (4)). In the following section, we provide a proof of concept for three other types of pollutants, including two types of bacteria, *E. coli* and *S. aureus*, the antibiotic tetracycline, and the industrial dye methylene blue.

Viruses are challenging to remove from water systems because of their small size, while bacteria can grow, replicate, form biofilms, repair damage, and adapt to their environment, meaning they may be more persistent in water systems when the disinfection method is not destructive enough (Lan et al., 2019). Gram-negative (G^-) *E. coli* and Gram-positive (G^+) *S. aureus* are standard strains for evaluating water disinfection performance (Duque-Sarango et al., 2023; Makarova et al., 2017).

Besides biological pollutants, chemical contamination of water also presents an issue with current water treatment techniques. Persistent chemicals with biological activity, like endocrine disruption, toxicity, antibiotic resistance, inflammation, and the like, can pose harmful consequences if not properly eliminated. TETR and MB are both persistent chemical pollutants that need to be removed from water by physical, chemical, or biological means due to their negative environmental impact (Slokar and Le Marechal, 1998). Standard wastewater treatment practices are sometimes inefficient or can result in large amounts of sludge (Robinson et al., 2001; W. Xu et al., 2007). Moreover, incomplete mineralisation can lead to the formation of some toxic byproducts (Ouzar and Kim, 2022; J. Wu et al., 2010), however there are some inconsistencies in the literature regarding byproducts toxicity of TC treatment with plasma (C. Fang et al., 2022; Ouzar and Kim, 2022). In detail, Ouzar et al. proposed that some byproducts may be more mutagenic than TC itself, while Fang et al. reported negligible biological toxicity of TC degradation byproducts. The effect of this can not be attributed to residual TC, since the study reporting biotoxicity had lower remaining TC concentrations after treatment than the other one (4.7 mg/L and 7 mg/L, respectively). Both studies used a software-based prediction approach (T.E.S.T.), while Fang et al. also evaluated toxicity towards bacteria *E. coli*, which showed no significant adverse effects. Here, H_2O_2 had been removed from the solution before carrying out the test, which may explain these discrepancies.

An ideal water treatment method should be able to degrade various types of pollutants, whether biological or chemical, as they are usually

present simultaneously in wastewater. Therefore, we conducted additional treatments of common wastewater pollutants to gain more insight into the effectiveness of the ICP plasma treatment method. The results are summarised in Fig. 12. Although the contaminants differ significantly, the trend is very similar: the treatment with V-UV radiation arising from hydrogen plasma in the H-mode efficiently destroys all these organic pollutants.

Different research teams used various experimental systems to evaluate the inactivation/degradation of bacteria, antibiotics, and organic dyes, so the results are not comparable, but the key difference between our approach and the brief state of the current knowledge as presented below is in the range of wavelengths used for UV and/or V-UV-assisted degradation of organic pollutants.

A broad subdivision of bacterial species to either G^- or G^+ stems from the latter having a thicker peptidoglycan cell wall (20–80 nm), allowing them to better retain the crystal violet staining dye (Coico, 2006). Since RONS initially interact and cause damage to the cell walls of microbes (Chen et al., 2021), it is reasonable to assume that G^- bacteria would be more susceptible to RONS disinfection techniques. This was indeed demonstrated by Kühn et al., using a UVA + TiO_2 disinfection method for producing $OH^\bullet$, and noting that the disinfection efficiency of various bacteria was correlated with the thickness of their respective cell walls (Kühn et al., 2003). Plasma-based techniques have previously been used to disinfect *E. coli*- or *S. aureus*-contaminated solutions, albeit on a small scale. Ma et al. used an atmospheric pressure DBD plasma to treat 50 μL of *E. coli* and *S. aureus* bacteria suspensions, achieving >6 $\log_{10}$ inactivation within 7 and 10 s, respectively (Ma et al., 2008). Similarly, Han et al. attempted to demonstrate the difference between direct versus indirect DBD plasma treatment. Interestingly, they obtained better inactivation of both *E. coli* and *S. aureus* with indirect rather than direct plasma treatment, which they attributed to long-lived RONS generated by the plasma discharge (L. Han et al., 2016).

Tetracycline, one of the most prolific antibiotics in human and veterinary medicine, is regularly detected in water systems due to its overuse, stability, and run-off to the environment (L. Xu et al., 2021), which may result in adverse effects on the biosphere (Amangelsin et al., 2023; Shutter and Akhondi, 2024). Standard treatment practices such as ozonation (J. Wu et al., 2010), UV treatment (Yuan et al., 2011) or their combination (F. Yang et al., 2024) have been shown to degrade TETR in wastewater, although the large-scale implementation of these methods has some disadvantages related to cost and/or efficiency (Antos et al., 2024). Research has been focused on developing new techniques for its expulsion from water systems. AOPs have been shown to efficiently degrade TETR only when O_3 was included in the treatment setup,

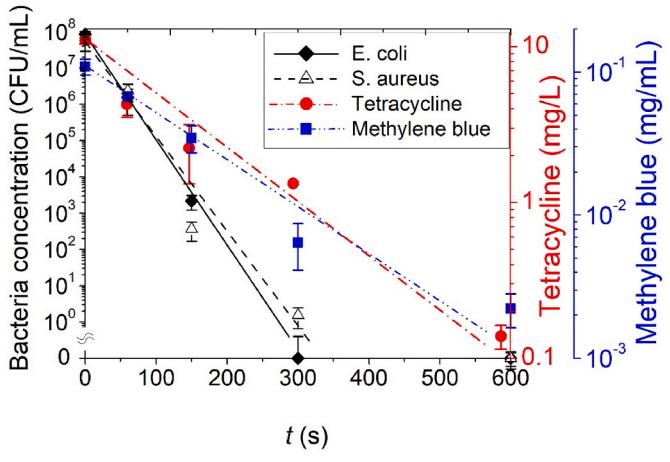

Fig. 12. V-UV treatment of common water pollutants, with plasma in the H-mode, air in the sample's treatment chamber headspace.

pointing to a strong correlation between TETR degradation and the presence of $OH^\bullet$, obtained from O_3 decomposition (Luu and Lee, 2014). Moreover, it was demonstrated by the same authors that the toxicity towards *E. coli* was lowered significantly after treatment, while the same was not observed in the *V. fischeri* bioluminescence assay, suggesting more research needs to be done to evaluate the generation of harmful by-products. Previously, atmospheric-pressure plasma treatment (He et al., 2014; Tang et al., 2018) and V-UV radiation (Krakkó et al., 2022; Yao et al., 2017) have been evaluated as methods for eliminating TETR from water. He et al. used a corona discharge in combination with a TiO_2 nano-catalyst, achieving an 85 % degradation after 24 min of treatment (He et al., 2014). Although the addition of a catalyst improved the degradation efficiency, a greater effect was demonstrated by increasing the plasma input power. On the other hand, 93 % of TETR was degraded by the dielectric barrier discharge plasma within 20 min of treatment (Tang et al., 2018). In both studies, it was postulated that the $OH^\bullet$ played a pivotal role in degrading TETR. V-UV radiation effectively degraded TETR from 650 mL solution within 10 min of treatment. Krakkó et al. demonstrated an increased degradation using UV/V-UV treatment of aqueous TETR, achieving complete degradation of 22.2 mg/L within 5 min. Additionally, possible degradation pathways and reactions were proposed, which aids in further optimisation of similar systems (Krakkó et al., 2022). A combined UV/V-UV process with adding a Fe (II) catalyst was able to degrade approximately 98 % of 8.8 mg/L of TETR within 30 min of treatment. With the 4-W cold-cathode low-pressure mercury lamp, the technique, according to the calculated EEO, was deemed cost-effective with 8.46 kWh/m^3 per order. The principal degradation agent was found to be the $OH^\bullet$ (Yao et al., 2017).

Paper and textile industries generate large amounts of wastewater, which are difficult to purify due to the amount and robustness of some pollutants. MB, a common dye in these industries, is a model compound for studying degradation kinetics and efficiency. Plasma has been employed several times to degrade this pollutant, with varying results. Although the authors are in general agreement that ROSs are the primary degradation factors, it is not as conclusive which is the primary one, as it varies between different setups. H_2O_2 was deemed the main degradation factor for alternating current- and microwave-excited atmospheric pressure plasma jets (Chandana et al., 2015; García et al., 2017), however, authors in both publications used pure argon gas for plasma generation, which is not ideal for ROS production besides H_2O_2 (Aboubakr et al., 2016; Bruggeman et al., 2016). When air or oxygen was supplied to the plasma gas mixture, a greater efficiency was achieved, which was attributed to a greater amount of ROS produced (B. Wang et al., 2017; L. Wu et al., 2019). A degradation pathway was proposed by Wu et al., who suspect that high energy electron, ozone, and hydroxyl radical are the primary main degradation agents for their atmospheric pressure DBD plasma reactor, however, they do not claim to have any V-UV radiation present, therefore these degradation mechanisms are not necessarily applicable to our system (L. Wu et al., 2019). One of the best reports of plasma MB degradation in water utilised an atmospheric-pressure dielectric barrier discharge air plasma. Large amounts (>50 mg/L) of H_2O_2 were generated, which were further converted to $OH^\bullet$ by the addition of a Fe (II), resulting in around 67 g/kWh degradation rate (Manoj Kumar Reddy et al., 2013).

4. Conclusion

Inductively coupled low-pressure plasma was used as a source of V-UV radiation in the range of wavelengths between about 150 and 200 nm. It is a highly versatile source of V-UV photons, which can produce various outcomes in a water treatment regime. Treatment parameters such as input power and the presence of oxygen at the gas-water interface have a profound effect on the efficiency of pollutant degradation, as showcased by an increase of $OH^\bullet$ generation, and pollutant degradation efficiency. With direct V-UV radiation in an oxygen atmosphere, the treatment was able to degrade 9 $\log_{10}$ of MS2 bacteriophage, 8 $\log_{10}$ of

E. coli and *S. Aureus* bacteria, as well as 10 mg/L of antibiotic tetracycline and 100 mg/L of industrial dye methylene blue, within 10 min of treatment time, all of which were remarkably concentrated, to demonstrate the potential of this method to treat highly polluted waters. Even though the energy of V-UV photons is large enough to disrupt the structure of viruses, causing their inactivation, it is the presence of oxygen at the gas-water interface that has the most significant effect on the overall production of $OH^{\bullet}$ and, subsequently, the inactivation of viruses. The experiments utilising a barrier for V-UV radiation showcase that some inactivation also occurs without direct interaction between the V-UV radiation and water. The insertion of the V-UV radiation barrier clearly showed that the gaseous radicals, created upon irradiation of air with V-UV photons, enter the water and contribute to virus inactivation, but the effect is smaller compared to the inactivation by $OH^{\bullet}$. The short- and long-lived RONS are thus inter-connected, being generated in either gas or liquid phase, and simultaneously carry out pollutant degradation, which would be interesting to investigate in future works. Some experiments were performed by adding the $OH^{\bullet}$ scavenger mannitol into the polluted water, and the results proved that the radicals play a prominent but not exclusive role in virus inactivation. However, the synergistic action of all the inactivation agents provides the best outcome, as long as the virus inactivation is the merit. In certain setups (E-mode, air), the EEO value (0.07 kWh/m^3/order) even outperformed some of the established water treatment methods, such as ozonation and UV-C irradiation (0.15 and 2 kWh/m^3/order, respectively), indicating that there is potential for this technique to be used as a water treatment method, especially when considering the range of different types of pollutants being effectively removed. Building on this proof-of-concept study, further work should evaluate the level of mineralisation, i.e., the amount of pollutant that is completely oxidised to CO_2 and H_2O, since degradation by-products may also pose health concerns when treated water is consumed or discharged. On a similar note, toxicological studies of treated water would be required, as harmful long-lived RONS may remain in liquid and cause harmful effects if not removed after treatment. One of the primary benefits of utilising V-UV in water treatment is its indiscriminate effectiveness against biological and chemical pollutants. However, its low penetration depth does necessitate a carefully designed setup to treat larger volumes of water, while optimizing energy efficiency could make this technique a valuable asset to the water treatment arsenal.

CRediT authorship contribution statement

Mark Zver: Writing – review & editing, Writing – original draft, Visualization, Methodology, Investigation, Formal analysis, Data curation, Conceptualization. **Rok Zaplotnik:** Writing – review & editing, Writing – original draft, Visualization, Validation, Methodology, Investigation, Formal analysis, Data curation. **Miran Mozetič:** Writing – review & editing, Investigation, Funding acquisition, Conceptualization. **Alenka Vesel:** Writing – review & editing, Validation, Methodology, Formal analysis, Data curation. **Arijana Filipić:** Writing – review & editing, Validation, Methodology. **David Dobnik:** Writing – review & editing, Validation, Supervision, Project administration. **Belisa Alcantara Marinho:** Writing – review & editing, Validation, Methodology, Investigation. **Gregor Primc:** Writing – review & editing, Writing – original draft, Visualization, Supervision, Project administration, Methodology, Funding acquisition, Conceptualization.

Declaration of competing interest

The authors declare the following financial interests/personal relationships which may be considered as potential competing interests: Mark Zver, Rok Zaplotnik, Miran Mozetic, Alenka Vesel, Arijana Filipić, David Dobnik, Belisa Alcantara Marinho reports financial support was provided by Slovenian Research and Innovation Agency. Gregor Primc reports financial support was provided by Slovenian Research and Innovation Agency. Belisa Alcantara Marinho reports financial support was provided by European Commission. If there are other authors, they declare that they have no known competing financial interests or personal relationships that could have appeared to influence the work reported in this paper.

Acknowledgements

The authors acknowledge the financial support from the Slovenian Research and Innovation Agency core fundings P2-0082, P4-0407, P2-0084, and project funding L2-2617.

B. Alcantara Marinho also acknowledges the European Commission for the HORIZON-WIDERA-2022-TALENTS270 02 grant agreement No. 101090289.

Data availability

Data will be made available on request.

References

Aboubakr, H.A., Gangal, U., Youssef, M.M., Goyal, S.M., Bruggeman, P.J., 2016. Inactivation of virus in solution by cold atmospheric pressure plasma: identification of chemical inactivation pathways. Journal of Physics D: Applied Physics 49 (20), 204001. https://doi.org/10.1088/0022-3727/49/20/204001.

Amangelsin, Y., Semenova, Y., Dadar, M., Aljofan, M., Bjørklund, G., 2023. The impact of tetracycline pollution on the aquatic environment and removal strategies. In Antibiotics 12 (Issue 3). https://doi.org/10.3390/antibiotics12030440. MDPI.

Anderson, C.E., Cha, N.R., Lindsay, A.D., Clark, D.S., Graves, D.B., 2016. The role of interfacial reactions in determining plasma–liquid chemistry. In Plasma Chemistry and Plasma Processing 36 (6), 1393–1415. https://doi.org/10.1007/s11090-016-9742-1.

Antos, J., Piosik, M., Ginter-Kramarczyk, D., Zembrzuska, J., Kruszelnicka, I., 2024. Tetracyclines contamination in European aquatic environments: a comprehensive review of occurrence, fate, and removal techniques. In Chemosphere 353. https://doi.org/10.1016/j.chemosphere.2024.141519. Elsevier Ltd.

Beck, N.K., Callahan, K., Nappier, S.P., Kim, H., Sobsey, M.D., Meschke, J.S., 2009. Development of a spot-titer culture assay for quantifying bacteria and viral indicators. Journal of Rapid Methods and Automation in Microbiology 17 (4), 455–464. https://doi.org/10.1111/j.1745-4581.2009.00182.x.

Beck, S.E., Ryu, H., Boczek, L.A., Cashdollar, J.L., Jeanis, K.M., Rosenblum, J.S., Lawal, O.R., Linden, K.G., 2017. Evaluating UV-C LED disinfection performance and investigating potential dual-wavelength synergy. Water Research 109, 207–216. https://doi.org/10.1016/j.watres.2016.11.024.

Bolton, J.R., Bircher, K.G., Tumas, W., Tolman, C.A., 2001. Figures of merit for the technical development and application of advanced oxidation technologies for both electric- and solar-driven systems † (IUPAC Technical Report). Pure Appl. Chem 73 (4).

Bruggeman, P.J., Kushner, M.J., Locke, B.R., Gardeniers, J.G.E., Graham, W.G., Graves, D.B., Hofman-Caris, R.C.H.M., Maric, D., Reid, J.P., Ceriani, E., Fernandez Rivas, D., Foster, J.E., Garrick, S.C., Gorbanev, Y., Hamaguchi, S., Iza, F., Jablonowski, H., Klimova, E., Kolb, J., et al., 2016. Plasma–liquid interactions: a review and roadmap. Plasma Sources Science and Technology 25 (5), 053002. https://doi.org/10.1088/0963-0252/25/5/053002.

Buchanan, W., Roddick, F., Porter, N., Drikas, M., 2004. Enhanced biodegradability of UV and VUV pre-treated natural organic matter. Water Science and Technology: Water Supply 4 (4), 103–111. https://doi.org/10.2166/ws.2004.0067.

Chabert, P., Tsankov, T.V., Czarnetzki, U., 2021. Foundations of capacitive and inductive radio-frequency discharges. Plasma Sources Science and Technology 30 (2). https://doi.org/10.1088/1361-6595/abc814.

Chandana, L., Manoj Kumar Reddy, P., Subrahmanyam, C., 2015. Atmospheric pressure non-thermal plasma jet for the degradation of methylene blue in aqueous medium. Chemical Engineering Journal 282, 116–122. https://doi.org/10.1016/j.cej.2015.02.027.

Chen, Y. di, Duan, X., Zhou, X., Wang, R., Wang, S., Ren, N. qi, Ho, S.H., 2021. Advanced oxidation processes for water disinfection: features, mechanisms and prospects. In Chemical Engineering Journal 409. https://doi.org/10.1016/j.cej.2020.128207. Elsevier B.V.

Coico, R., 2006. Gram staining. Current Protocols in Microbiology 00 (1). https://doi.org/10.1002/9780471729259.mca03cs00.

Duque-Sarango, P., Romero-Martínez, L., Pinos-Vélez, V., Sánchez-Cordero, E., Samaniego, E., 2023. Comparative study of UV radiation resistance and reactivation characteristics of E. coli ATCC 8739 and native strains: implications for water disinfection. Sustainability (Switzerland) 15 (12). https://doi.org/10.3390/su15129559.

Fang, C., Wang, S., Xu, H., Huang, Q., 2022. Degradation of tetracycline by atmospheric-pressure non-thermal plasma: enhanced performance, degradation mechanism, and toxicity evaluation. Science of the Total Environment 812. https://doi.org/10.1016/j.scitotenv.2021.152455.

Fang, J., Liu, H., Shang, C., Zeng, M., Ni, M., Liu, W., 2014. E. coli and bacteriophage MS2 disinfection by UV, ozone and the combined UV and ozone processes. Frontiers of Environmental Science & Engineering 8 (4), 547–552. https://doi.org/10.1007/s11783-013-0620-2.

Förster, F., 2022. Atmospheric pressure plasma in industrial applications: surface treatment of thermally sensitive polymers. Plasma Processes and Polymers 19 (Issue 10). https://doi.org/10.1002/ppap.202100240. John Wiley and Sons Inc.

García, M.C., Mora, M., Esquivel, D., Foster, J.E., Rodero, A., Jiménez-Sanchidrián, C., Romero-Salguero, F.J., 2017. Microwave atmospheric pressure plasma jets for wastewater treatment: degradation of methylene blue as a model dye. Chemosphere 180, 239–246. https://doi.org/10.1016/j.chemosphere.2017.03.126.

Goldstein, S., Czapski, G., 1984. Mannitol as an OH· scavenger in aqueous solutions and in biological systems. International Journal of Radiation Biology and Related Studies in Physics, Chemistry and Medicine 46 (6), 725–729. https://doi.org/10.1080/09553008414551961.

Gonzalez, M.C., Braun, A.M., 1995. VUV photolysis of aqueous solutions of nitrate and nitrite. Research on Chemical Intermediates 21 (8–9), 837–859. https://doi.org/10.1163/156856795X00512.

Gonzalez, M.G., Oliveros, E., Wörner, M., Braun, A.M., 2004. Vacuum-ultraviolet photolysis of aqueous reaction systems. Journal of Photochemistry and Photobiology C: Photochemistry Reviews 5 (3), 225–246. https://doi.org/10.1016/j.jphotochemrev.2004.10.002.

Gosar, Ž., Kovač, J., Mozetič, M., Primc, G., Vesel, A., Zaplotnik, R., 2020. Characterization of gaseous plasma sustained in mixtures of HMDSO and O2 in an industrial-scale reactor. Plasma Chemistry and Plasma Processing 40 (1), 25–42. https://doi.org/10.1007/s11090-019-10026-5.

Guo, L., Xu, R., Gou, L., Liu, Z., Zhao, Y., Liu, D., Zhang, L., Chen, H., Kong, M.G., 2018. Mechanism of virus inactivation by cold atmospheric-pressure plasma and plasma-activated water. Applied and Environmental Microbiology 84 (17). https://doi.org/10.1128/AEM.00726-18.

Halfmann, H., Denis, B., Bibinov, N., Wunderlich, J., Awakowicz, P., 2007. Identification of the most efficient VUV/UV radiation for plasma based inactivation of Bacillus atrophaeus spores. Journal of Physics D: Applied Physics 40 (19), 5907–5911. https://doi.org/10.1088/0022-3727/40/19/019.

Han, L., Patil, S., Boehm, D., Milosavljević, V., Cullen, P.J., Bourke, P., 2016. Mechanisms of inactivation by high-voltage atmospheric cold plasma differ for Escherichia coli and Staphylococcus aureus. Applied and Environmental Microbiology 82 (2), 450–458. https://doi.org/10.1128/AEM.02660-15.

Han, W., Zhang, P., Zhu, W., Yin, J., Li, L., 2004. Photocatalysis of p-chlorobenzoic acid in aqueous solution under irradiation of 254 nm and 185 nm UV light. Water Research 38 (19), 4197–4203. https://doi.org/10.1016/j.watres.2004.07.019.

He, D., Sun, Y., Xin, L., Feng, J., 2014. Aqueous tetracycline degradation by non-thermal plasma combined with nano-TiO2. Chemical Engineering Journal 258, 18–25. https://doi.org/10.1016/j.cej.2014.07.089.

Hoigné, J., Bader, H., 1976. The role of hydroxyl radical reactions in ozonation processes in aqueous solutions. Water Research 10 (5), 377–386. https://doi.org/10.1016/0043-1354(76)90055-5.

Hull, N.M., Linden, K.G., 2018. Synergy of MS2 disinfection by sequential exposure to tailored UV wavelengths. Water Research 143, 292–300. https://doi.org/10.1016/j.watres.2018.06.017.

Imoberdorf, G.E., Mohseni, M., 2011. Experimental study of the degradation of 2,4-D induced by vacuum-UV radiation. Water Science and Technology 63 (7), 1427–1433. https://doi.org/10.2166/wst.2011.321.

Jiang, B., Zheng, J., Qiu, S., Wu, M., Zhang, Q., Yan, Z., Xue, Q., 2014. Review on electrical discharge plasma technology for wastewater remediation. Chemical Engineering Journal 236, 348–368. https://doi.org/10.1016/j.cej.2013.09.090.

Joshi, A.A., Locke, B.R., Arce, P., Finney, W.C., 1995. Formation of hydroxyl radicals, hydrogen peroxide and aqueous electrons by pulsed streamer corona discharge in aqueous solution. Journal of Hazardous Materials 41.

Kanarik, K.J., 2020. Inside the mysterious world of plasma: a process engineer's perspective. Journal of Vacuum Science & Technology A 38 (3). https://doi.org/10.1116/1.5141863.

Kanazawa, S., Kawano, H., Watanabe, S., Furuki, T., Akamine, S., Ichiki, R., Ohkubo, T., Kocik, M., Mizeraczyk, J., 2011. Observation of OH radicals produced by pulsed discharges on the surface of a liquid. Plasma Sources Science and Technology 20 (3). https://doi.org/10.1088/0963-0252/20/3/034010.

Krakkó, D., Heieren, B.T., Illés, Á., Kvamme, K., Dóbé, S., Záray, G., 2022. (V)UV degradation of the antibiotic tetracycline: kinetics, transformation products and pathway. Process Safety and Environmental Protection 163, 395–404. https://doi.org/10.1016/j.psep.2022.05.027.

Krakkó, D., Illés, Á., Licul-Kucera, V., Dávid, B., Dobosy, P., Pogonyi, A., Demeter, A., Mihucz, V.G., Dóbé, S., Záray, G., 2021. Application of (V)UV/O3 technology for post-treatment of biologically treated wastewater: a pilot-scale study. Chemosphere 275, 130080. https://doi.org/10.1016/j.chemosphere.2021.130080.

Kühn, K.P., Chaberny, I.F., Massholder, K., Stickler, M., Benz, V.W., Sonntag, H.G., Erdinger, L., 2003. Disinfection of surfaces by photocatalytic oxidation with titanium dioxide and UVA light. Chemosphere 53 (1), 71–77. https://doi.org/10.1016/S0045-6535(03)00362-X.

Lan, L., Zhang, R., Zhang, X., Shi, H., 2019. Sublethal injury and recovery of Listeria monocytogenes and Escherichia coli O157:H7 after exposure to slightly acidic electrolyzed water. Food Control 106. https://doi.org/10.1016/j.foodcont.2019.106746.

Lee, C., Kim, J., Yoon, J., 2011. Inactivation of MS2 bacteriophage by streamer corona discharge in water. Chemosphere 82 (8), 1135–1140. https://doi.org/10.1016/j.chemosphere.2010.11.036.

Legrini, O., Oliveros, E., Braun, A.M., 1993. Photochemical processes for water treatment. Chemical Reviews 93 (2), 671–698. https://doi.org/10.1021/cr00018a003.

Liu, Y., Ogden, K., 2010. Benefits of high energy UV185nm light to inactivate bacteria. Water Science and Technology 62 (12), 2776–2782. https://doi.org/10.2166/wst.2010.200.

Luu, H.T., Lee, K., 2014. Degradation and changes in toxicity and biodegradability of tetracycline during ozone/ultraviolet-based advanced oxidation. Water Science and Technology 70 (7), 1229–1235. https://doi.org/10.2166/wst.2014.350.

Ma, Y., Zhang, G.J., Shi, X.M., Xu, G.M., Yang, Y., 2008. Chemical mechanisms of bacterial inactivation using dielectric barrier discharge plasma in atmospheric air. IEEE Transactions on Plasma Science 36 (4 PART 3), 1615–1620. https://doi.org/10.1109/TPS.2008.917165.

Makarova, O., Johnston, P., Walther, B., Rolff, J., Roesler, U., 2017. Complete Genome Sequence of the Disinfectant Susceptibility Testing Reference Strain Staphylococcus aureus subsp. aureus ATCC 6538. https://doi.org/10.1128/genomeA.

Manoj Kumar Reddy, P., Rama Raju, B., Karuppiah, J., Linga Reddy, E., Subrahmanyam, C., 2013. Degradation and mineralization of methylene blue by dielectric barrier discharge non-thermal plasma reactor. Chemical Engineering Journal 217, 41–47. https://doi.org/10.1016/j.cej.2012.11.116.

Matafonova, G., Batoev, V., 2022. Dual-wavelength light radiation for synergistic water disinfection. Sci. Total Environ. 806, 151233. https://doi.org/10.1016/j.scitotenv.2021.151233.

Miklos, D.B., Remy, C., Jekel, M., Linden, K.G., Drewes, J.E., Hübner, U., 2018. Evaluation of advanced oxidation processes for water and wastewater treatment – a critical review. In Water Research 139, 118–131. https://doi.org/10.1016/j.watres.2018.03.042. Elsevier Ltd.

Moldgy, A., Aboubakr, H., Nayak, G., Goyal, S., Bruggeman, P., 2020. Comparative evaluation of the virucidal effect of remote and direct cold air plasmas with UV-C. Plasma Processes and Polymers 17 (4), 1900234. https://doi.org/10.1002/ppap.201900234.

Ochiai, T., Masuko, K., Tago, S., Nakano, R., Niitsu, Y., Kobayashi, G., Horio, K., Nakata, K., Murakami, T., Hara, M., Nojima, Y., Kurano, M., Serizawa, I., Suzuki, T., Ikekita, M., Morito, Y., Fujishima, A., 2013. Development of a hybrid environmental purification unit by using of excimer VUV lamps with TiO2 coated titanium mesh filter. Chemical Engineering Journal 218, 327–332. https://doi.org/10.1016/j.cej.2012.12.048.

Oladoye, P.O., Ajiboye, T.O., Omotola, E.O., Oyewola, O.J., 2022. Methylene blue dye: toxicity and potential elimination technology from wastewater. Results in Engineering 16, 100678. https://doi.org/10.1016/j.rineng.2022.100678.

Ouzar, A., Kim, I.K., 2022. Tetracycline degradation by nonthermal plasma: removal efficiency, degradation pathway, and toxicity evaluation. Water Science and Technology 86 (11), 2794–2807. https://doi.org/10.2166/wst.2022.339.

Prasad, M.N.V., Grobelak, A., 2020. In: Prasad, M.V.N., Grobelak, A. (Eds.), Waterborne Pathogens: Detection and Treatment. Butterworth-Heinemann.

Ramsay, I.A., Niedziela, J.-C., Ogden, I.D., 2000. The synergistic effect of excimer and low-pressure mercury lamps on the disinfection of flowing. Water 1529–1533. https://doi.org/10.4315/0362-028x-63.11.1529.

Reisz, E., Schmidt, W., Schuchmann, H.P., Von Sonntag, C., 2003. Photolysis of ozone in aqueous solutions in the presence of tertiary butanol. Environmental Science and Technology 37 (9), 1941–1948. https://doi.org/10.1021/es0113100.

Robinson, T., McMullan, G., Marchant, R., Nigam, P., 2001. Remediation of dyes in textile effluent: a critical review on current treatment technologies with a proposed alternative. Bioresource Technology 77 (3), 247–255. https://doi.org/10.1016/S0960-8524(00)00080-8.

Sahni, M., Locke, B.R., 2006. Quantification of hydroxyl radicals produced in aqueous phase pulsed electrical discharge reactors. Industrial and Engineering Chemistry Research 45 (17), 5819–5825. https://doi.org/10.1021/ie0601504.

Schlemm, H., Fritzsche, M., Roth, D., 2005. Linear radio frequency plasma sources for large scale industrial applications in photovoltaics. Surface and Coatings Technology 200 (1–4), 958–961. https://doi.org/10.1016/j.surfcoat.2005.05.020.

Sherchan, S.P., Snyder, S.A., Gerba, C.P., Pepper, I.L., 2014. Inactivation of MS2 coliphage by UV and hydrogen peroxide: comparison by cultural and molecular methodologies. Journal of Environmental Science and Health - Part A Toxic/Hazardous Substances and Environmental Engineering 49 (4), 397–403. https://doi.org/10.1080/10934529.2014.854607.

Shutter, M.C., Akhondi, H., 2024. Tetracycline. In StatPearls 9 (Issue 12). StatPearls Publishing. http://www.ncbi.nlm.nih.gov/pubmed/16443056.

Slokar, Y.M., Le Marechal, A.M., 1998. Methods of decoloration of textile wastewaters. Dyes and Pigments 37 (4).

Tang, S., Yuan, D., Rao, Y., Zhang, J., Qu, Y., Gu, J., 2018. Evaluation of antibiotic oxytetracycline removal in water using a gas phase dielectric barrier discharge plasma. Journal of Environmental Management 226, 22–29. https://doi.org/10.1016/j.jenvman.2018.08.022.

Tendero, C., Tixier, C., Tristant, P., Desmaison, J., Leprince, P., 2006. Atmospheric pressure plasmas: a review. In Spectrochimica Acta - Part B Atomic Spectroscopy 61 (1), 2–30. https://doi.org/10.1016/j.sab.2005.10.003. Elsevier.

Tigrine, S., Carrasco, N., Vettier, L., Cernogora, G., 2016. A microwave plasma source for VUV atmospheric photochemistry. Journal of Physics D: Applied Physics 49 (39). https://doi.org/10.1088/0022-3727/49/39/395202.

Venkatramani, N., 2002. Industrial plasma torches and applications. Current Science 83 (Issue 3).

Vesel, A., Zaplotnik, R., Mozetič, M., Recek, N., 2023. Advanced method for efficient functionalization of polymers by intermediate free-radical formation with vacuum-ultraviolet radiation and producing superhydrophilic surfaces. Journal of

Photochemistry and Photobiology A: Chemistry 443. https://doi.org/10.1016/j.jphotochem.2023.114876.

Wang, B., Dong, B., Xu, M., Chi, C., Wang, C., 2017. Degradation of methylene blue using double-chamber dielectric barrier discharge reactor under different carrier gases. Chemical Engineering Science 168, 90–100. https://doi.org/10.1016/j.ces.2017.04.027.

Wang, D., Oppenländer, T., El-Din, M.G., Bolton, J.R., 2010. Comparison of the disinfection effects of vacuum-UV (VUV) and UV light on Bacillus subtilis spores in aqueous suspensions at 172, 222 and 254 nm. Photochemistry and Photobiology 86 (1), 176–181. https://doi.org/10.1111/j.1751-1097.2009.00640.x.

Watanabe, K., Inn, E.C.Y., Zelikoff, M., 1953. Absorption coefficients of oxygen in the vacuum ultraviolet. The Journal of Chemical Physics 21 (6), 1026–1030. https://doi.org/10.1063/1.1699104.

Wu, J., Jiang, Y., Zha, L., Ye, Z., Zhou, Z., Ye, J., Zhou, H., 2010. Tetracycline degradation by ozonation, and evaluation of biodegradability and toxicity of ozonation byproducts. Canadian Journal of Civil Engineering 37 (11), 1485–1491. https://doi.org/10.1139/L10-100.

Wu, L., Xie, Q., Lv, Y., Wu, Z., Liang, X., Lu, M., Nie, Y., 2019. Degradation of methylene blue via dielectric barrier discharge plasma treatment. Water (Switzerland) 11 (9). https://doi.org/10.3390/w11091818.

Wu, Y., Liang, Y., Wei, K., Li, W., Yao, M., Zhang, J., Grinshpun, S.A., 2015. MS2 virus inactivation by atmospheric-pressure cold plasma using different gas carriers and power levels. Applied and Environmental Microbiology 81 (3), 996–1002. https://doi.org/10.1128/AEM.03322-14.

Xu, L., Zhang, H., Xiong, P., Zhu, Q., Liao, C., Jiang, G., 2021. Occurrence, fate, and risk assessment of typical tetracycline antibiotics in the aquatic environment: a review. In Science of the Total Environment 753. https://doi.org/10.1016/j.scitotenv.2020.141975. Elsevier B.V.

Xu, W., Zhang, G., Li, X., Zou, S., Li, P., Hu, Z., Li, J., 2007. Occurrence and elimination of antibiotics at four sewage treatment plants in the Pearl River Delta (PRD), South China. Water Research 41 (19), 4526–4534. https://doi.org/10.1016/j.watres.2007.06.023.

Yang, F., Wang, D., Zhang, X., Zhang, J., Wu, Z., Wang, Q., 2024. Synergistic effects of peroxydisulfate on UV/O3 process for tetracycline degradation: mechanism and pathways. Chinese Chemical Letters 35 (10). https://doi.org/10.1016/j.cclet.2024.109599.

Yang, Z.-C., Wang, W.-L., Jing, Z.-B., Jiang, Y.-Q., Zhang, H.-Q., Lee, M.-Y., Peng, L., Wu, Q.-Y., 2024. Ozone, hydrogen peroxide, and peroxymonosulfate disinfection of MS2 coliphage in water. Environmental Science: Processes & Impacts 26 (5), 824–831. https://doi.org/10.1039/D3EM00527E.

Yao, H., Pei, J., Wang, H., Fu, J., 2017. Effect of Fe(II/III) on tetracycline degradation under UV/VUV irradiation. Chemical Engineering Journal 308, 193–201. https://doi.org/10.1016/j.cej.2016.09.074.

Yuan, F., Hu, C., Hu, X., Wei, D., Chen, Y., Qu, J., 2011. Photodegradation and toxicity changes of antibiotics in UV and UV/H2O2 process. Journal of Hazardous Materials 185 (2–3), 1256–1263. https://doi.org/10.1016/j.jhazmat.2010.10.040.

Zaplotnik, R., Vesel, A., Mozetic, M., 2011. Transition from e to H mode in inductively coupled oxygen plasma: Hysteresis and the behaviour of oxygen atom density. EPL 95 (5). https://doi.org/10.1209/0295-5075/95/55001.

Zhou, R., Zhou, R., Wang, P., Xian, Y., Mai-Prochnow, A., Lu, X., Cullen, P.J., Ostrikov, K., Ken, Bazaka, K., 2020. Plasma-activated water: generation, origin of reactive species and biological applications. Journal of Physics D: Applied Physics 53 (30), 303001. https://doi.org/10.1088/1361-6463/ab81cf.

Zver, M., Zaplotnik, R., Mozetič, M., Vesel, A., Filipić, A., Dobnik, D., Primc, G., 2025. Characterization of low-pressure gaseous plasma radiation and its usage for inactivation of waterborne viruses. Separation and Purification Technology 354. https://doi.org/10.1016/j.seppur.2024.128691.